ADVANCED FUNCTIONAL MATERIALS
www.afm-journal.de

Materials Views
www.MaterialsViews.com

FULL PAPER

Fluorene-Based Asymmetric Bipolar Universal Hosts for White Organic Light Emitting Devices

Ejabul Mondal, Wen-Yi Hung, Hung-Chi Dai, and Ken-Tsung Wong**

Two new bipolar host molecules composed of hole-transporting carbazole and electron-transporting cyano (CzFCN) or oxadiazole (CzFOxa)-substituted fluorenes are synthesized and characterized. The non-conjugated connections, via an sp^3-hybridized carbon, effectively block the electronic interactions between electron-donating and -accepting moieties, giving CzFCN and CzFOxa bipolar charge transport features with balanced mobilities (10^{-5} to 10^{-6} cm^2 V^{-1} s^{-1}). The *meta–meta* configuration of the fluorene-based acceptors allows the bipolar hosts to retain relatively high triplet energies [$E_T = 2.70$ eV (CzFOxa) and 2. 86 eV (CzFCN)], which are sufficiently high for hosting blue phosphor. Using a common device structure – ITO/PEDOT:PSS/DTAF/TCTA/host:10% dopants (from blue to red)/DPPS/LiF/Al – highly efficient electrophosphorescent devices are successfully achieved. CzFCN-based devices demonstrate better performance characteristics, with maximum η_{ext} of 15.1%, 17.9%, 17.4%, 18%, and 20% for blue (FIrpic), green [$(PPy)_2Ir(acac)$], yellowish-green [*m*-$(Tpm)_2Ir(acac)$], yellow [$(Bt)_2Ir(acac)$], and red [$Os(bpftz)_2(PPhMe_2)_2$, OS1], respectively. In addition, combining yellowish-green *m*-$(Tpm)_2Ir(acac)$ with a blue emitter (FIrpic) and a red emitter (OS1) within a single emitting layer hosted by bipolar CzFCN, three-color electrophosphorescent WOLEDs with high efficiencies (17.3%, 33.4 cd A^{-1}, 30 lm W^{-1}), high color stability, and high color-rendering index (CRI) of 89.7 can also be realized.

1. Introduction

Phosphorescent organic light-emitting devices (PhOLEDs) are of extensive research interest in academia and industry because of their potential applications in full-color flat-panel displays and thin-film lighting.[1] Due to the strong spin-orbit coupling, PhOLEDs with heavy metal-centered phosphors can efficiently harvest both the singlet and triplet excitons, thus enabling a 100% internal quantum efficiency (IQE).[2] In order to achieve unity IQE, the suppression of detrimental effects of phosphors, such as aggregation quenching and triplet–triplet annihilation, is essential. Therefore, the host–guest strategy has been commonly used in PhOLEDs with triplet emitters (guest) homogeneously dispersed within suitable host materials. In this regard, the developments of new host materials are as important as the design of efficient triplet emitters with promising characters for realizing the practical applications of PhOLEDs. The host materials play an important role for charge transport and electron/hole balance as well as confinement of emissive excitons in the emissive layer, which are important factors responsible for high-efficiency PhOLEDs.[3] One promising molecular design strategy of host materials to achieve high and balanced electric flux is to incorporate electron-donating (D) and electron-accepting (A) components into a single bipolar molecule, thereby facilitating injection and transport of holes and electrons into the emitting layer.[4] However, the bipolar host material hybridizing the individual characteristics of D and A moieties should avoid efficient intramolecular charge transfer to give triplet energy higher than the phosphor to prevent reverse energy transfer from guest to host.[5] This becomes more challenging for host materials used in blue phosphorescent emitter. To preserve high triplet energy, the interruption of the π-conjugation between D and A components in a bipolar molecule by using highly-twisted or saturated spacers is crucial.[4] For cost-effective fabrication of full-color PhOLED displays, it is highly desired that the host material is concurrently suitable for red (R), green (G), and blue (B) phosphors with the same device structure to give high electroluminescence (EL) efficiencies for individual emitting colors. In addition, by combining two or three appropriate efficient phosphorescent emitters, all-phosphor white organic light-emitting diodes (WOLEDs) using a universal host material can also be reasonably achieved. Therefore, efforts are ongoing for the development of universal bipolar host materials with high triplet energy (≥2.7 eV) suitable for various phosphors in high-efficiency PhOLEDs. Nevertheless, the reported host materials concurrently suitable for RGB phosphors are relatively limited.[6] For example, Cheng recently reported a universal bipolar host material bis-[4-(*N*-carbazolyl)phenyl]phenylphosphine oxide (BCPO) containing a phosphine oxide as acceptor and two carbazole groups as donor exhibiting promising properties,[6a] which can be applied as an efficient host for blue, green, and red

---

Dr. E. Mondal, Prof. K.-T. Wong
Department of Chemistry
National Taiwan University
Taipei 10617, Taiwan (R.O.C.)
E-mail: kenwong@ntu.edu.tw
Prof. W.-Y. Hung, H.-C. Dai
Institute of Optoelectronic Sciences
National Taiwan Ocean University
Keelung 202, Taiwan (R.O.C.)
E-mail: wenhung@mail.ntou.edu.tw

DOI: 10.1002/adfm.201202889

phosphorescent devices with extremely high external quantum efficiencies (η_{ext}). Recently, we reported a new bipolar host CMesB by incorporating dimesityl borane at the C3 and C6 positions of *N*-phenylcarbazole.[6e] PhOLEDs using CMesB as host doped with various emitters yield η_{ext} of 20.7% for red, 20.0% for green, 16.5% for blue, and 15.7% for white OLEDs at practical brightness. However, these excellent hosts usually adopted different device structures for individual dopants for giving optimal device performance. The reported universal bipolar host materials suitable for various phosphors under the same device architecture are relatively rare. One elegant example was reported by Yang, where a bipolar host *p*-BISiTPA comprising silicon-bridged triphenylamine (D) and benzimidazole (A) moieties, giving a high triplet energy (E_T) of 2.69 eV and bipolar transporting features.[6b] Devices employing *p*-BISiTPA as host exhibited η_{ext} as high as 16.1% for blue, 22.7% for green, 20.5% for orange, and 19.1% for all-phosphor (two-color) WOLEDs under a common device structure. Recently, we reported a universal bipolar host CNBzIm with high T_g of 180 °C and triplet energy ($E_T = 2.71$ eV), by incorporating electron-accepting *N*-phenylbenzimidazole units via *N*-bridge connection at the C3 and C6 positions of *N*-phenylcarbazole.[6d] PhOLEDs employing CNBzIm as a host doped with various phosphors under the same device structure show excellent performance, with η_{ext} as high as 12.7% for blue, 17.8% for green, 19.1% for red. A two-color, all-phosphor, and single-emitting-layer WOLEDs hosted by CNBzIm was also achieved with maximum efficiencies of 15.7%, 35 cd A^{-1}, and 36.6 lm W^{-1}.

In this paper, we report two bipolar host materials **CzFCN** and **CzFOxa** (**Scheme 1**), in which the C9 of fluorene was adopted as the nonconjugated bridge to connect hole-transporting carbazole as donor and C3-substituted fluorenes as acceptor. An electron-withdrawing cyano group was selected as acceptor because it can enhance both the electron affinity for efficient electron injection and electron transport.[7] In addition, the oxadiazole group, derivatized easily from the cyano group, is a well-established electron-transporting (ET) functional group used in OLEDs.[8] Obviously, direct electronic interactions between donor and acceptor(s) can be efficiently blocked with a saturated spacer (C9 of fluorene). In addition, the *meta*–*meta* configurations of the acceptor moieties ensure limited extension of π-conjugation for preserving high triplet energies. Moreover, the presence of a tolyl group makes the C9 position of fluorene a chirality center, leading the resultant bipolar molecule to be a racemic mixture, which we believe will ensure an amorphous character and thus thin-film stability of the emitting layer. These two novel hosts were suitable for various phosphorescent emitters, including FIrpic, $(PPy)_2Ir(acac)$, $(Bt)_2Ir(acac)$, $Os(bpftz)_2(PPhMe_2)_2$,and a new yellowish-green emitter bis-(*m*-totylpyrimidine)(acetylacetonate)iridium(III) (*m*-$(Tpm)_2Ir(acac)$; see Scheme S1 in the Supporting Information, SI) with excellent device performance. PhOLEDs employing **CzFCN** as a host doped with RGB phosphors under the common device structure of ITO/PEDOT:PSS (30 nm)/DTAF (20 nm)/TCTA (5 nm)/CzFCN:10% dopant (25 nm)/DPPS (50 nm)/LiF/Al with η_{ext} as high as 15.1% for blue, 17.9% for green, 17.4% for yellowish-green, 18% for yellow, and 20% for red were achieved. More importantly, **CzFCN**-hosted devices demonstrated remarkable stability with a low efficiency roll-off at a brightness of 1000 cd m^{-2}. On the other hand, devices with **CzFOxa** as host using the same device structure provided good performance with η_{ext} of 9.2% for blue, 14.5% for green, 16.2% for yellowish-green, 17.6% for yellow, and 19.4% for red, respectively. In addition, by combining a new yellowish-green emitter *m*-$(Tpm)_2Ir(acac)$ with a blue emitter (FIrpic) and a red emitter (OS1), three-color, all-phosphor, and single emitting layer WOLEDs hosted by **CzFCN** and **CzFOxa** were obtained with three evenly separated main RGB peaks with maximum η_{ext} of 17.3% and 15.7%, power efficiencies (η_p) of 30 lm W^{-1}, 28 lm W^{-1}, respectively, and a high color-rendering index (CRI) of up to 89. The WOLEDs exhibited high color stabilities owing to broad charge recombination zones within the emitting layer incorporated within these novel bipolar hosts.

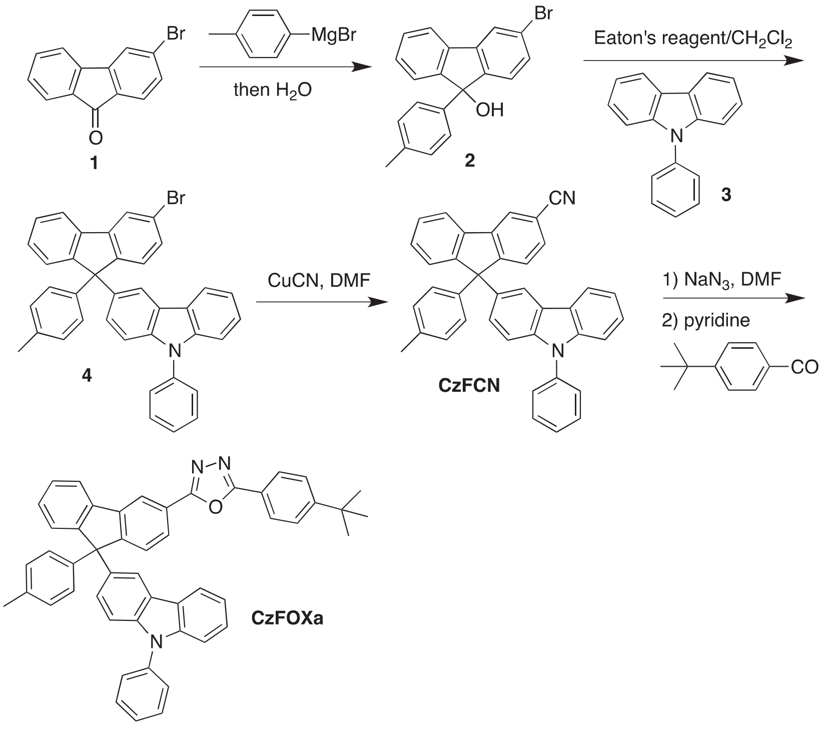

Scheme 1. Synthetic routes to **CzFCN** and **CzFOxa**.

2. Results and Discussion

2.1. Synthesis and Characterization

Scheme 1 illustrates our synthetic routes towards **CzFCN and CzFOxa.** The reaction of 3-bromofluorenone (**1**)[9] with the Grignard reagent 4-bromotoluene gave the corresponding alcohol 3-bromo-9-*p*-tolyl-9H-fluoren-9-ol (**2**) in 93% yield. 9-Phenylcarbazole **3** was treated with alcohol **2** in CH_2Cl_2 using Eaton's reagent[10] as the catalyst and

Table 1. Physical properties of **CzFCN and CzFOxa**.

Host	T_g [°C]	T_d [°C]	$E_{1/2}^{OX}$ [V]	$E_{1/2}^{RED}$ [V]	HOMO [eV][a)]	LUMO [eV][b)]	ΔE_g [eV][c)]	E_T [eV]	Abs λ_{max} [nm]solid/film	PL λ_{max} [nm]solid/film
CzFCN	134	335	1.35	– 2.21	– 5.65	– 2.18	3.47	2.86	243,298/243,300	357,373/357
CzFOxa	170	406	1.35	– 1.99	– 5.8	– 2.45	3.35	2.70	285,331/285,336	415/390

[a)] HOMO determined using photoelectron yield spectroscopy (AC-2); [b,c)] LUMO is determined from the equation LUMO = HOMO + E_g, where E_g was calculated from the absorption onset of the solid film.

condensing agent at room temperature, giving **4** in 73% isolated yield after column chromatography. Bipolar host **CzFCN** was obtained in 60% yield as compound **4** was reacted with CuCN in dimethylformamide (DMF) and refluxed for 24 h at 148 °C. Bipolar host **CzFOxa** was synthesized from **CzFCN**. **CzFCN** treated with NaN_3 and NH_4Cl in DMF at 100 °C gave tetrazole intermediate **5** in 90% yield, which was subsequently treating with 4-*tert*-butylbenzoyl chloride in pyridine to afford **CzFOxa** in 80% yield. All the intermediates and **CzFCN**, **CzFOxa** were fully characterized using ^1H and ^{13}C NMR spectroscopy, mass spectrometry, and elemental analysis (see the experimental section in the SI). In addition, a new pyrimidine-based green phosphor, *m*-(Tpm)$_2$Ir(acac), was synthesized (see Scheme S1 in the SI). The photophysical and electrochemical properties of m-(Tpm)$_2$Ir(acac) are shown in Figures S1 and S2, respectively, and summarized in Table S1 in SI.

2.2. Thermal Properties

The morphological and thermal properties of bipolar hosts **CzFCN** and **CzFOxa** were investigated by differential scanning calorimetry (DSC) and thermogravimetric analysis (TGA; **Table 1**). Host materials **CzFCN** and **CzFOxa** exhibited high glass transition temperatures (T_g) of 134 and 170 °C, respectively. In addition, no crystallization or melt was detected at the second heating. Their decomposition temperatures were recorded at 335 and 406 °C, respectively (T_d; corresponding to 5% weight loss). The amorphous behavior of **CzFCN** and **CzFOxa** can be reasonably attributed to the character of racemic mixture. The high T_g and T_d values of **CzFOxa** as compared to **CzFCN** are presumably because of higher molecular weight. The good thermal stability with high T_g is beneficial for these host materials to form homogeneous and amorphous films, verified by the atomic force microscopic (AFM) analyses shown in Figure S3 in the SI, which are crucial for successful use in thin-film devices by vacuum deposition.

2.3. Photophysical Properties

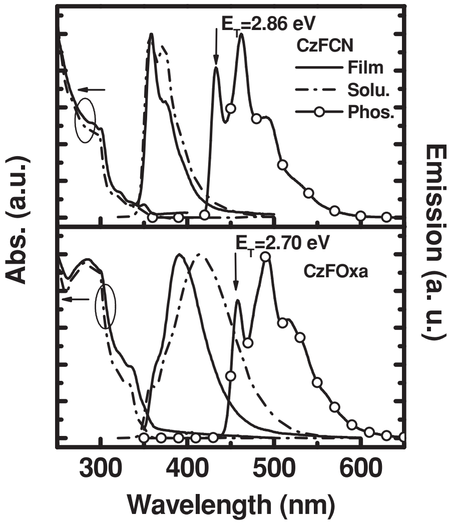

Figure 1. Room-temperature absorption and emission (PL) spectra of **CzFCN** and **CzFOxa** in CH_2Cl_2 and neat films as well as corresponding phosphorescence (Phos) spectra recorded in EtOH at 77 K.

Figure 1 presents the UV-vis absorption and emission (PL) spectra of **CzFCN** and **CzFOxa** in dilute solution (CH_2Cl_2) and neat films. The photophysical data are summarized in Table 1. The absorption peak of **CzFCN** around 300 nm could be assigned to the π–π* transition, while weak shoulder peaks at 326 and 350 nm are attributed to the n–π* transitions of carbazole. The emission of **CzFCN** showed clear vibronic feature with maximum centered at λ_{max} 357 nm. As compared to those of **CzFCN**, **CzFOxa** exhibit red-shifted absorption (332 nm) and emission (415 nm) spectra due to the extended π-conjugation along with oxadiazole substitution. To gain more insight into the photophysical properties, we studied the emission behavior of **CzFCN** and **CzFOxa** in various solutions (1×10^{-5}M) (see Figure S4 to S7 in the SI). The evident solvatochromic behavior of **CzFOxa** indicates the occurrence of photoinduced intramolecular charge transfer (ICT), leading to a polar excited state which was sensitive to the polarity of solvents. In contrast, the limited changes in the emission spectra of **CzFCN** in different solvents reveal the ineffective ICT behavior.[11] Apparently, the introduction of oxadiazole onto the fluorene core leads to a lower lowest unoccupied molecular orbital (LUMO) level, giving a good tendency for an efficient ICT between the carbazole donor and oxadiazole-substituted acceptor. The phosphorescence spectra of **CzFCN** and **CzFOxa** were measured in EtOH at 77 K and the triplet energies (E_T) were estimated, from the highest energy vibronic band of the phosphorescence spectra, to be 2.86 and 2.70 eV, respectively. The high triplet energy of **CzFCN** is comparable to previously reported host material,[12] revealing that the introduction of a CN group at the C3 position of the fluorene unit has a weak effect on increasing the E_T due to the *meta–meta* configuration. However, the introduced oxadiazole in **CzFOxa** has evident influence on the resultant

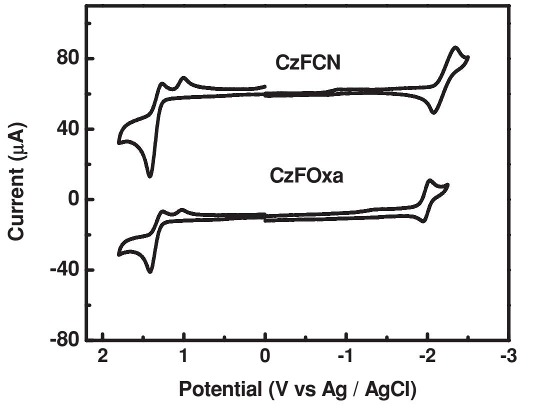

Figure 2. Cyclic voltammogram of **CzFCN** and **CzFOxa**. The measurement of oxidation potentials were performed in CH_2Cl_2 with 0.1 M of $n$$Bu_4NPF_6$ as a supporting electrolyte, and the reduction CV were performed in tetrahydrofuran (THF)/DMF with 0.1 M of $n$$Bu_4NClO_4$ as a supporting electrolyte.

bipolar molecule. Nevertheless, the triplet energies of **CzFCN** and **CzFOxa** are sufficiently high to serve as host materials for various RGB triplet emitters.

2.4. Electrochemical Properties

Cyclic voltammetry (CV) was performed to study the electrochemical properties of bipolar host materials **CzFCN** and **CzFOxa** (**Figure 2**). The electrochemical data of **CzFCN** and **CzFOxa** are summarized in Table 1. The observed irreversible oxidation behaviors of **CzFCN** and **CzFOxa** at 1.35 V (vs. Ag/AgCl) are typical for C3, C6–unprotected 9-phenylcarbazole, while the new low potential peaks at 1.01 V (vs. Ag/AgCl) indicate the dimerization of carbazole.[13] On the other hand, both **CzFCN** and **CzFOxa** exhibited a well-defined quasi-reversible reduction process at –2.21 and –1.99 V (vs. Ag/AgCl), respectively, arising from the cyano- and oxadiazole-substituted fluorene. The elctrochemical properties of **CzFCN** and **CzFOxa** clearly indicated their bipolarity, revealing the potential hole/electron transport properties in OLED devices. By using a Ricken AC-2 photoemission spectrometer, we determined the highest occupied molecular orbital (HOMO) energy level of **CzFCN** and **CzFOxa** to be –5.65 and –5.80 eV, respectively. From the equation LUMO = HOMO + ΔE_g, where ΔE_g is the optical bandgap determined from the absorption threshold, we estimated the LUMO energy level of **CzFCN** and **CzFOxa** to be –2.18 and –2.45 eV, respectively.

2.5. Charge-Carrier Mobility

In order to confirm the bipolar transporting properties of **CzFCN** and **CzFOxa**, we used time-of-flight (TOF) techniques to measure the associated carrier mobility.[14] The device used for TOF measurement was prepared through vacuum deposition of the tri-layer structure as: ITO glass/**CzFCN** (1.76 μm) or **CzFOxa** (2.07 μm)/Ag (150 nm), followed by placing them inside a vacuum chamber for data measurement. **Figure 3**a–d display typical room-temperature TOF transients for both materials under an applied electric field, for which we observed typical transient photocurrents from both holes and electrons. Using double-logarithmic representations (insets to Figure 3a–d), we extracted the carrier-transit times (t_T), which are required to determine the carrier mobilities, from the intersections of the two asymptotes. We then calculated the mobility using the formula $\mu = d^2/Vt_T$, where d is the sample thickness and V is the applied voltage. **Figure 4** shows the carrier mobilities of **CzFCN** and **CzFOxa** plotted as a function of the square root of the applied electric field, as well as the nearly universal Poole-Frenkel relationship. The electron mobilities of **CzFCN** lie in the range 1.1×10^{-5} to 2.4×10^{-5} cm^2 V^{-1} s^{-1} for fields varying from 5.1×10^5 to 8.0×10^5 V cm^{-1}; these are higher than the hole mobilities, which are within the range 3.6×10^{-6} to 1.2×10^{-5} cm^2 V^{-1} s^{-1} for fields varying from 4.0×10^5 to 6.8×10^5 V cm^{-1}. This tendency is very similar to those of **CzFOxa**: the electron mobilities lie in the range 3.3×10^{-6} to 9.3×10^{-6} cm^2 V^{-1} s^{-1} for fields varying from 2.9×10^5 to 5.8×10^5 V cm^{-1}, and the hole mobilities in the range 1.4×10^{-6} to 4.4×10^{-6} cm^2 V^{-1} s^{-1} for fields varying from 1.9×10^5 to 5.8×10^5 V cm^{-1}. These results indicate that the **CzFCN** and **CzFOxa** show bipolar charge-transport properties with balance electron/hole mobilities. However, the hole- and electron-mobilities of **CzFCN** are ca. two-times greater than those of **CzFOxa**. This can be attributed to the attachment of less bulky electron-withdrawing cyano onto fluorene results in close molecular

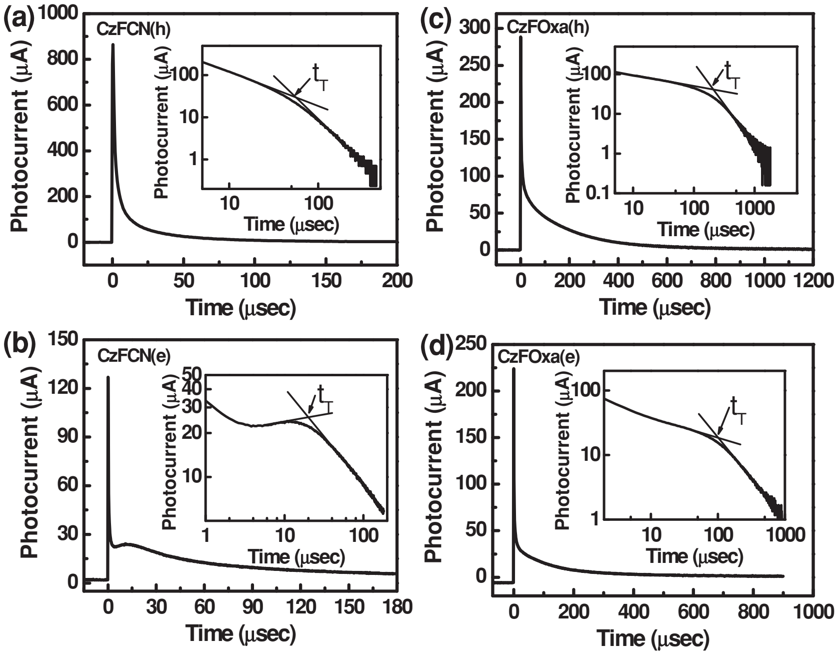

Figure 3. Typical transient photocurrent signals for **CzFCN** (1.76 μm thick) at $E = 5.7 \times 10^5$ V cm^{-1} and **CzFOxa** (2.07 μm thick) at $E = 3.9 \times 10^5$ V cm^{-1}:a,c) holes, and, b,d) electrons. Insets are the corresponding double logarithmic plots.

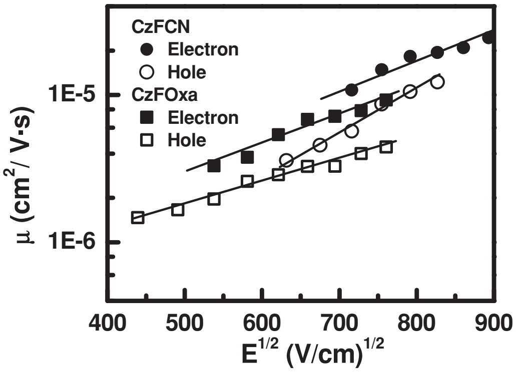

Figure 4. Electron and hole mobilities versus $E^{1/2}$ for **CzFCN** and **CzFOxa**.

packings than the bulky oxadiazole in **CzFOxa**, which induce easier carrier hopping among the adjacent molecules.

2.6. Monochromatic Devices

To evaluate the applications of bipolar molecules **CzFCN** and **CzFOxa** as host materials, we fabricated blue, green, yellow-green, yellow, and red electrophosphorescent devices using Iridium(III)[bis(4,6-difluorophenyl)-pyridinato-*N*,$C^{2'}$] picolinate (FIrpic),[15] bis(2-phenylpyridinato)iridium(III) acetylacetonate [$(PPy)_2Ir(acac)$],[16] bis(*m*-tolylpyrimidine)iridium(III) acetylacetonate [*m*-$(Tpm)_2Ir(acac)$], bis(2-phenylbenzothiazolato) (acetylacetonate)iridium(III) [$(Bt)_2Ir(acac)$],[17] and osmium(II) bis[3-(trifluoromethyl)-5-(4-*tert*-butylpyridyl)-1,2,4-triazolate] dimethylphenylphosphine [$Os(bpftz)_2(PPhMe_2)_2$, OS1][18] as dopants (**Scheme 2**), respectively, in the structure: ITO/poly ethylenedioxythiophene:polystyrenesulfonate (PEDOT:PSS, 30 nm)/9,9-di[4-(di-*p*-tolyl)aminophenyl]fluorene (DTAF, 20 nm)[19]/4,4′,4″-tri(*N*-carbazolyl)triphenylamine (TCTA, 5 nm)[20]/host:dopant (10 wt-%, 25 nm)/diphenyl-bis[4-(pyridin-3-yl)phenyl]silane (DPPS, 50 nm)[21]/LiF (0.5 nm)/Al (100 nm). To maximize PhOLED efficiency, a high E_T hole-transporter (HTL) and electron-transporter (ETL) are also imperative to prevent any possible luminescence quenching by the carrier-transporting layers and to confine the triplet excitons in the EML. As shown in our previous report, DTAF with a high triplet level (E_T = 2.87 eV) and wide bandgap (E_g = 3.47 eV) can efficiently confine the triplet energy of phosphors, is selected as the HTL.[19] TCTA, (E_T: 2.76 eV; HOMO/LUMO: 5.7/2.4 eV) is selected to act as both triplet exciton blocker and HTL to stepwise reduce the hole injection barrier from DTAF to EML. To further confine

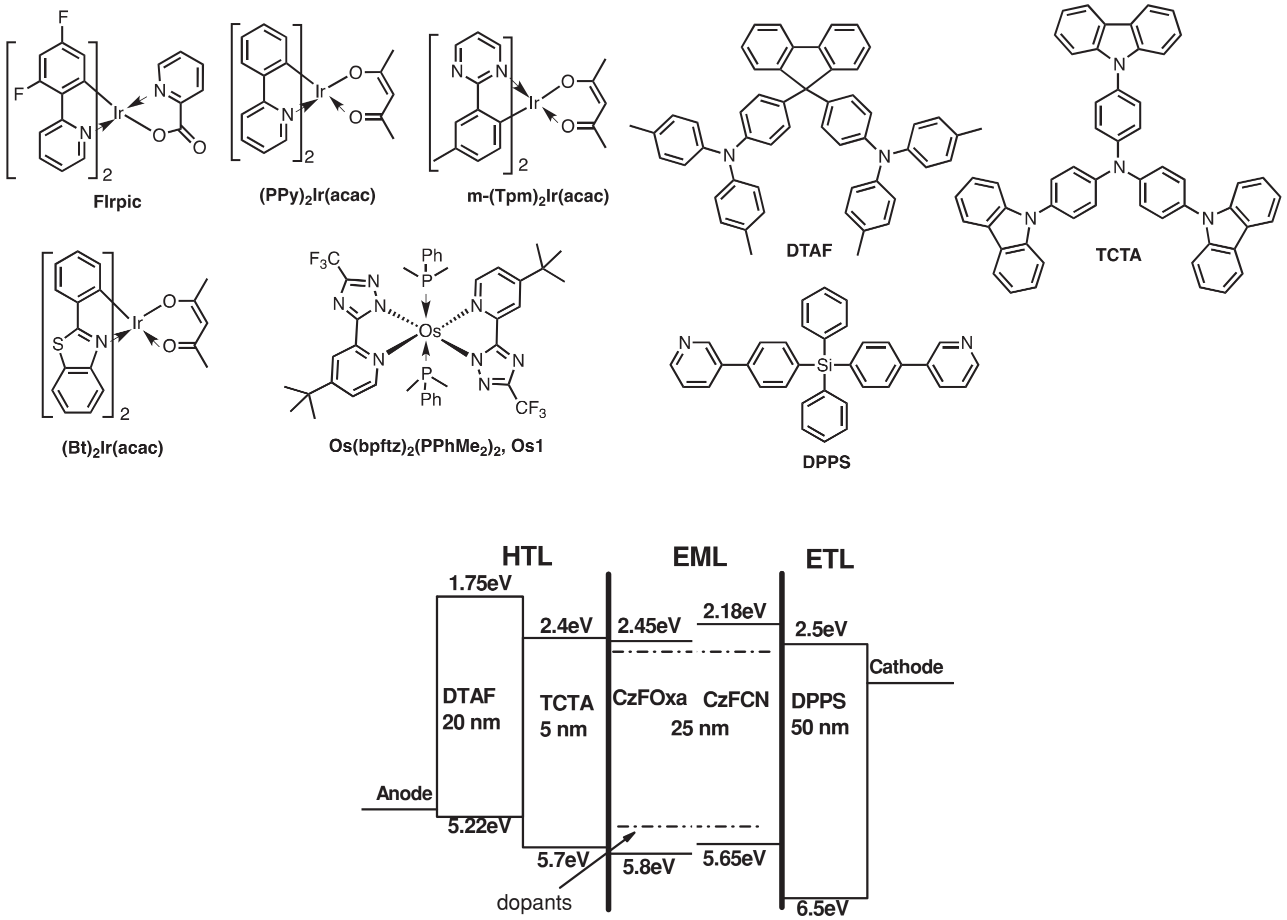

Scheme 2. Molecular structures used in this study and an energy level diagram of the device.

Table 2. EL performance of devices.

	V_{on} [V][b]	L_{max} [cd m^{-2}]	J_{max} [mA cm^{-2}]	η_{ext} [%]	η_c [cd A^{-1}]	η_p [lm W^{-1}]	η_{ext} [V,%][c]	CIE [x,y]
B1[a]	2.5	38 200 (14 V)	520	15.1	31.6	18.5	7.8, 15.1	0.17,0.35
G1	2.5	150 600 (14 V)	920	17.9	64.7	60	6.0, 17.9	0.35,0.62
YG1	2.5	103 000 (15 V)	850	17.4	60.4	40	6.5, 17.4	0.43,0.56
Y1	2.5	80 600 (16.5 V)	690	18	44.1	34	8.5, 17.1	0.53,0.47
R1	2.5	26 200 (16.5 V)	650	20	21.8	20	8.5, 17.3	0.65,0.35
W1	2.5	54 300 (14.5 V)	760	17.3	33.4	30	8.0, 14.2	0.45,0.43
B2	2.5	35 300 (13.5 V)	800	9.2	22	19.2	6.6, 8.9	0.18,0.39
G2	2.5	160 000 (14.5 V)	1170	14.5	53.2	50	5.0, 14.4	0.35,0.62
YG2	2.5	126 600 (14.5 V)	920	16.2	53.6	53.2	6.0, 14.5	0.42,0.56
Y2	2.5	99 600 (15 V)	1020	17.6	45.4	47.5	6.2, 13.3	0.52,0.48
R2	2.5	32 300 (13.5 V)	890	19.4	21.3	22.3	6.5, 16.5	0.65,0.34
W2	2.5	47 000 (13 V)	790	15.7	31.2	28	7.5, 12.3	0.46,0.43
B3[d]	3.0	45 300 (15.5 V)	720	17.7	35.6	22.5	7.1, 17.3	0.16,0.33
Y3[d]	2.5	162 300 (14 V)	1090	14.0	48.2	22.3	5.7, 11.5	0.35,0.61
R3[d]	3.0	24 800 (14.5 V)	630	15.7	15.0	7.6	7.6, 15.7	0.64,0.35

[a] The notation 1 and 2 indicate the devices fabricated with host materials of **CzFCN** and **CzFOxa**, respectively; [b] Turn-on voltage at which emission became detectable; [c] η_{ext} and driving voltage of device at 1000 cd m^{-2}; [d] For comparison, references cell with emitting layer of mCP:FIrpic (B3), CBP:(PPy)$_2$Ir(acac) (G3), and CBP:OS1 (R3) were fabricated with the same device structure.

the holes or generated excitons within the emissive region, DPPS (E_T: 2.7 eV; HOMO/LUMO: 6.5/2.5 eV) is selected as the ETL to block the excitons within the EML. PEDOT:PSS, LiF, and Al served as hole-, electron-injecting layer, and cathode, respectively. For comparison, we made reference cells utilizing the known host materials mCP (doped with FIrpic) and CBP [doped with (PPy)$_2$Ir(acac) and OS1] as emitting layer (**Table 2** and Figure S8 in the SI).

Figure 5 and **6** show the current density–voltage–brightness (*J*–*V*–*L*) characteristics, efficiency versus brightness curves, and EL spectra of the devices. The key characteristics of the devices are listed in Table 2. All devices displayed low turn-on voltage at 2.5 V. The devices hosted by **CzFOxa** exhibited significantly higher current density and lower driving voltage (at 1000 cd m^{-2}) than that of **CzFCN**, which is due to more efficient electron injection in EML/ETL interface. As compared to the reference cells, the **CzFCN**-hosted blue device was comparable to the mCP-hosted one (device **B3**). Both the **CzFCN**- and **CzFOxa**-hosted devices outperformed the BCP-hosted devices (devices **Y3** and **R3**).

The blue emission device **B1** hosted by **CzFCN** reveals a maximum brightness (L_{max}) of 38 200 cd m^{-2} at 14 V (520 mA cm^{-2}) with CIE coordinates of (0.17, 0.35). The maximum external quantum (η_{ext}), current (η_c), and power efficiencies (η_p) were 15.1%, 31.6 cd A^{-1}, and 18.5 lm W^{-1}, respectively, which are significantly higher than those for **CzFOxa** based device **B2** (9.2%, 22 cd A^{-1}, and 19.2 lm W^{-1}). At a high brightness of 1000 cd m^{-2}, the η_{ext} of devices **B1** and **B2** are still as high as 15.1% and 8.9%, respectively, showing very low efficiency roll-off. The η_{ext} of the **CzFCN** device was over 50% higher than that of the **CzFOxa** device. This can be attributed to the higher E_T of **CzFCN** compared with **CzFOxa**, efficiently suppressing triplet energy back transfer from the guest to the host and consequently resulting in efficient blue electrophosphorescence for the **CzFCN**-based device. The same trend can be observed for devices **G1** and **G2** using (PPy)$_2$Ir(acac) as dopant. The device **G1** exhibited an L_{max} of 150 600 cd m^{-2} at 14 V with CIE coordinates of (0.35, 0.62) and attractive EL efficiencies (17.9%, 64.7cd A^{-1}, 60 lm W^{-1}) that are superior to those of the device **G2** (14.5%, 53.2 cd A^{-1}, 50 lm W^{-1}). At a high brightness of 1000 cd m^{-2}, the η_{ext} of devices **G1** and **G2** are still as high as 17.9% and 14.4%, respectively, also showing very low efficiency roll-off.

For yellowish-green emission, we synthesized a new yellowish-green emitter, *m*-(Tpm)$_2$Ir(acac) by modified the ligands of (Tpm)$_2$Ir(acac). As depicted in Figure S9 (see the SI), the EL spectrum originated from the triplet emission of *m*-(Tpm)$_2$Ir(acac) with a central electroluminescence wavelength (λ_{EL}) of 547 nm and CIE coordinates of (0.43, 0.56), which was red-shifted (ca. 11 nm) compared to the (Tpm)$_2$Ir(acac)-based device [λ_{EL} = 536 nm, CIE coordinates of (0.43, 0.56)]. It was noted that the efficiency of the devices incorporating **CzFCN** with *m*-(Tpm)$_2$Ir(acac) was significantly higher than that of the devices with (Tpm)$_2$Ir(acac). For example, at a brightness of 1000 cd m^{-2}, the η_{ext} of device with *m*-(Tpm)$_2$Ir(acac) reached 17.4%, which is 1.05 times higher than the 16.5% found for the devices with (Tpm)$_2$Ir(acac) (see Table S2 in the SI). In addition, we also compared **CzFCN** with **CzFOxa** as host in *m*-(Tpm)$_2$Ir(acac)-based devices. Device **YG1** hosted by **CzFCN** displays substantially higher efficiencies (17.4%, 60.4 cd A^{-1}, and 40 ml W^{-1}) than device **YG2** hosted by **CzFOxa** (16.2%, 53.6 cd A^{-1}, and 53.2 ml W^{-1}). Remarkably, the device **YG1** shows rather low efficiency roll-off at a brightness of 1000 cd m^{-2},

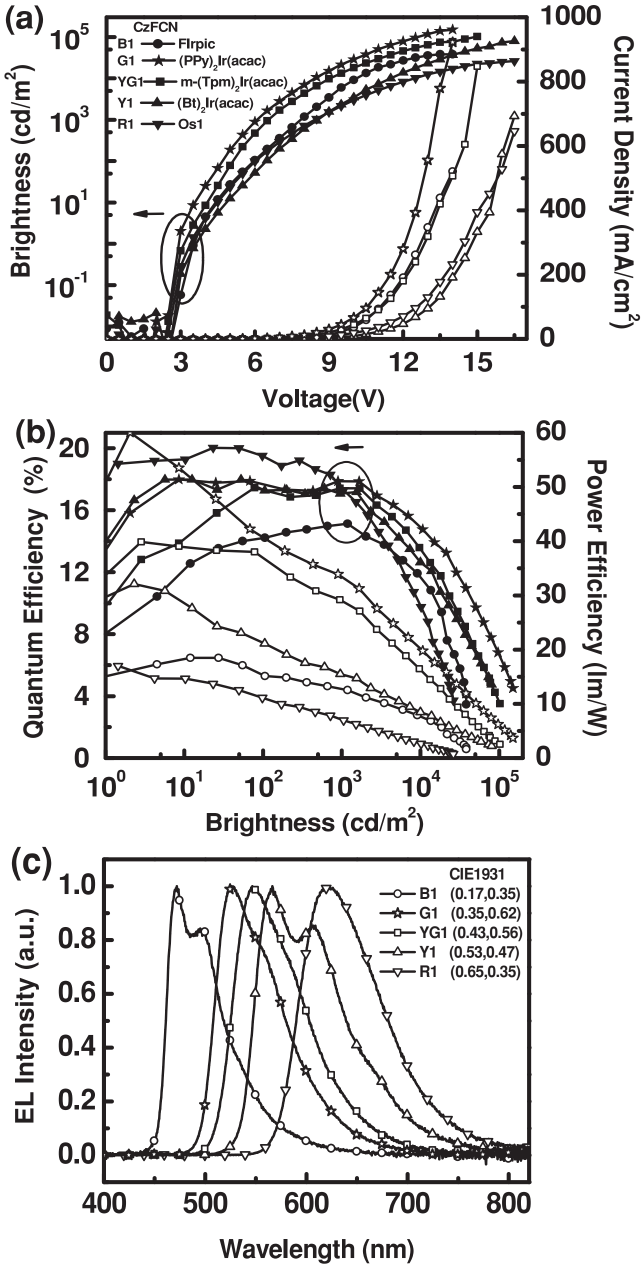

Figure 5. a) Current density–voltage–luminance (*J–V–L*) characteristics. b) External quantum (η_{ext}) and power efficiencies (η_P) as a function of brightness. c) EL spectra of devices for **CzFCN** as host.

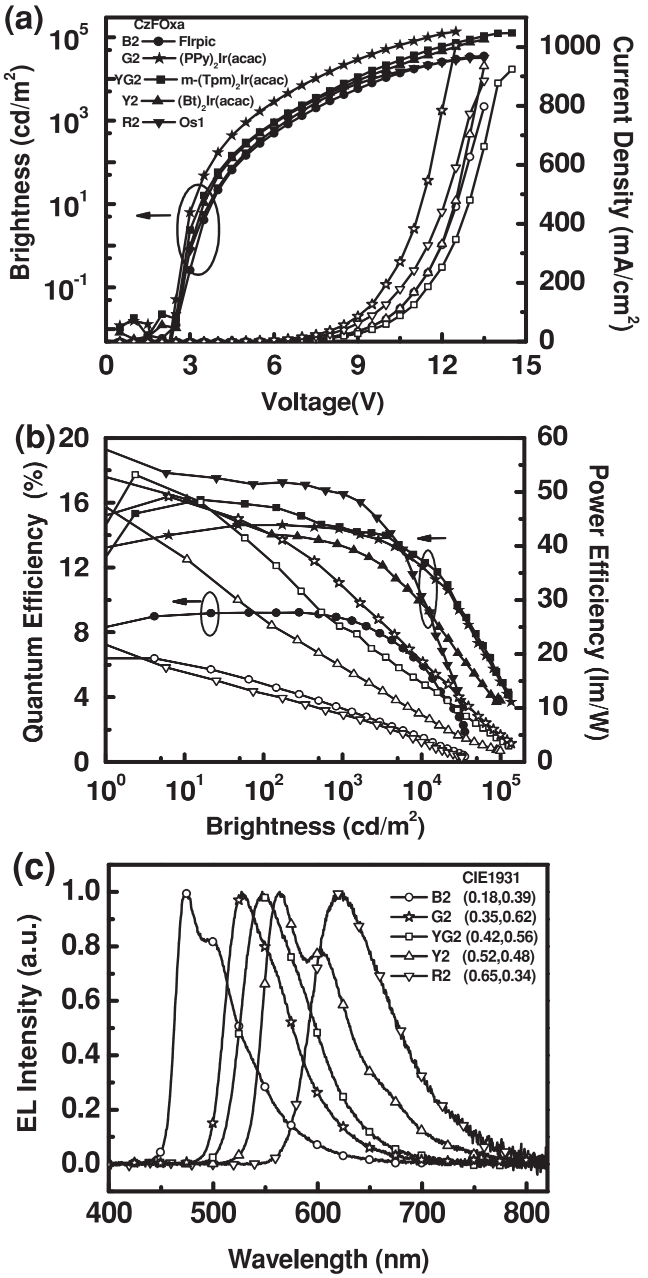

Figure 6. a) Current density–voltage–luminance (*J–V–L*) characteristics. b) External quantum (η_{ext}) and power efficiencies (η_P) as a function of brightness. c) EL spectra of devices for **CzFOxa** as host.

while the recorded η_{ext} is still maintained as high as 17.4%. These values are comparable to those of the best yellowish-green phosphorescent OLEDs in the literature.[22] The emission color and excellent performance of *m*-(Tpm)$_2$Ir(acac) suggest the good potential of employing *m*-(Tpm)$_2$Ir(acac) as the emitter for the construction of efficient WOLEDs showing evenly separated R, G, and B colors.

Next, yellow-emitting PhOLEDs were fabricated using (Bt)$_2$Ir(acac) as dopant (device **Y1** and **Y2**). Both devices exhibit high performance. For instance, the device **Y1** exhibited an L_{max} of 80 600 cd m^{-2} at 690 mA cm^{-2} (16.5 V) and very good EL efficiencies (18%, 44.1 cd A^{-1}, and 34 lm W^{-1}) with the CIE coordinates of (0.53, 0.47) while the device **Y2** exhibited an L_{max} of 99 600 cd m^{-2} at 1020 mA cm^{-2} (15 V) and respectable EL efficiencies (17.6%, 45.4 cd A^{-1}, and 47.5 lm W^{-1}) with the CIE coordinates of (0.52, 0.48). It is notable that, at a practical brightness of 1000 cd m^{-2}, the η_{ext} of device **Y1** remained as high as 17.1%, which is higher than that of 13.3% observed for **Y2**. The problem of the rapid efficiency roll-off in the device was greatly improved in the device hosted by **CzFCN**. As a result, the present phosphors may serve as potential emitting elements for generating white light in combination with a complementary blue phosphor.

Finally, we demonstrated red-emitting PhOLEDs using the emitter Os1 (device **R1** and **R2**), which exhibited excellent EL performance. For instance, the device **R1** exhibited an L_{max} of 26 200 cd m^{-2} at 650 mA cm^{-2} (16.5 V) and excellent EL efficiencies (20%, 21.8 cd A^{-1}, and 20 lm W^{-1}) with CIE coordinates of (0.65, 0.35) while the device **R2** exhibited an L_{max} of 32 300 cd m^{-2} at 13.5 V and very good EL efficiencies (19.4%, 21.3 cd A^{-1}, and 22.3 lm W^{-1}) with the CIE coordinates of (0.65, 0.34). The devices displayed relatively pure emission and there are no residual emissions from the host and/or adjacent layers in Figure 5c and 6c, indicating that the electroluminescence is solely originated from the Os1 dopant and with completed energy transfer from host to dopant. Considering the out-coupling factor, this reaches nearly 100% internal efficiency. All these devices from blue to red emission revealed very low turn-on voltage (2.5 V) and excellent performances were obtained from the same device architecture incorporated with different phosphors. It is fascinating to mention that by using **CzFCN** as the universal host, the performance of these basic-color devices is comparable to the best one that have been reported.[23,6a–c]

2.7. Single-Host WOLEDs with RGB Colors

WOLEDs have been attracting particular attention because of their potential application in solid-state lighting. Nevertheless, how to improve device efficiency, color stability track-off, and color-rendering index (CRI) are the critical demands of commercial lighting applications. Various approaches have been reported to improve phosphorescent WOLED performance, which include doping of two or three phosphors that emit B–R complementary colors or R–G–B primary colors in single- or multi-emitting layers.[24] Among them, mutli-EMLs containing R–G–B phosphors can improve device efficiency, color stability, and CRI by precisely controlling exciton/charge distribution in the devices. Here, we fabricated WOLEDs (device **W1** and **W2**) by distributing the R–G–B primary color emitters in multiple regions within a single-host (**CzFCN** and **CzFOxa**), which can reduce structural heterogeneity and facilitate charge injection and transport between different emissive centers. The WOLEDs have similar architecture as the aforementioned monochromatic devices except for EML [host: 10% FIrpic (5 nm)/host: 10% *m*-(Tpm)$_2$Ir(acac) (5 nm)/host:10% OS1 (5 nm)/host: 10% FIrpic (10 nm)]. FIrpic is a sky-blue emitter with a central emission wavelength of 473 nm while OS1 is a red emitter with a central emission wavelength of 619 nm. In order to generate the white spectrum with three evenly separated R, G, and B peaks, we selected *m*-(Tpm)$_2$Ir(acac) (peak at 547 nm) as the green emitter. The emission spectra of the emitters compensate each other so that the white spectrum generated can cover the whole visible region.

Figure 7 shows the *J–V–L* characteristics and curves of external quantum efficiency and power efficiency versus brightness. The EL characteristics of white devices are also summarized in Table 2. The turn-on voltages of devices **W1** and **W2** are ca. 2.5 V, almost the same as those of the monochromatic devices, suggesting that the insertion of the mutli-EMLs did not influence the effective charge injection and transportation. Device **W1** hosted by **CzFCN** achieves an L_{max} of 54 300 cd m^{-2} at 760 mA cm^{-2} (14.5 V), and excellent EL efficiencies (17.3%, 33.4 cd A^{-1}, and 30 lm W^{-1}). Device **W1**'s efficiencies are higher than those of the comparable device **W2** using **CzFOxa** as host (15.7%, 31.2 cd A^{-1}, and 28 lm W^{-1}), which is probably because device **W1** exhibited a higher blue emission. In addition, the EL spectra of devices **W1** and **W2** cover all wavelengths from 450 to 800 nm (**Figure 8**), and the color-rendering index (CRI) is calculated to reach as high as 89. The spectra also demonstrated highly stable chromaticity (CIEx = 0.45–0.43 and CIEy = 0.43) for device **W1** and (CIEx = 0.46–0.47 and CIEy = 0.43) for device **W2** at applied voltage of 7 to 11 V. The efficient WOLEDs with separated R, G, and B peaks and a high CRI of up to 89, would be ideal candidates to bring OLEDs into the next generation of full-color displays and the solid-state lighting market.

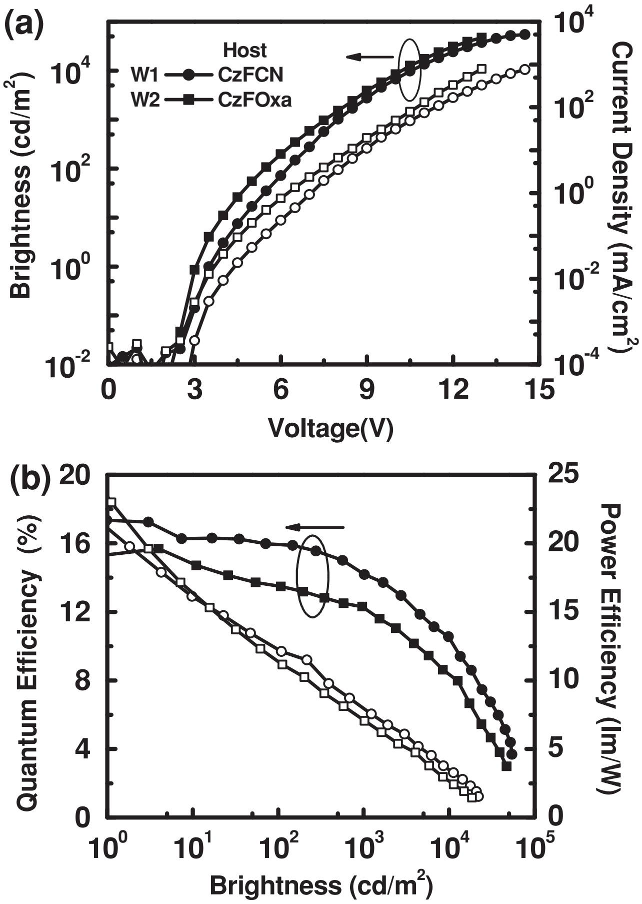

Figure 7. a) Current density-voltage-luminance (*J–V–L*) characteristics. b) External quantum (η_{ext}) and power efficiencies (η_P) as a function of brightness of white devices.

3. Conclusions

Two new bipolar host molecules **CzFCN** and **CzFOxa** composed of electron-rich carbazole linked through a sp^3-hybridized carbon bridge to electron-deficient cyano or oxadiazole-substituted fluorenes were synthesized and characterized. The electronic interactions between two functional constituents were

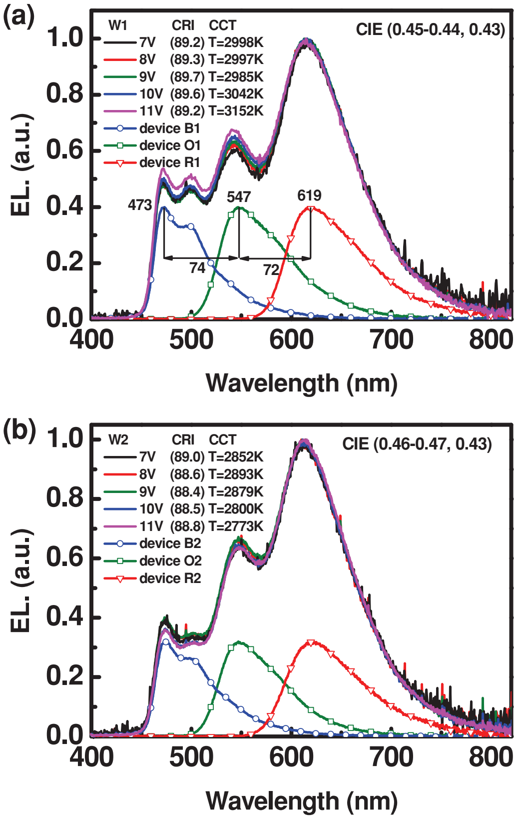

Figure 8. The normalized EL spectra of white devices by hosted a) **CzFCN** and b)**CzFOxa** at various voltages.

effectively blocked, giving **CzFCN** and **CzFOxa** sufficiently high triplet energy, morphological stabilities, and bipolar character with balanced charge mobilities. These promising characters render **CzFCN** and **CzFOxa** feasible to realize highly efficient and low roll-off red/green/blue PhOLEDs adopting a common device configuration. In addition, single-host WOLEDs with R–G–B colors can be realized to give outstanding efficiency and CRI, in particular showing superior color stability. Our results clearly indicated that tailor-made bipolar host materials concurrently suitable for red (R), green (G), and blue (B) phosphors for cost-effective fabrications of full-color PhOLED displays and WOLED light sources can be reasonably achieved.

Supporting Information

Supporting Information is available from the Wiley Online Library or from the author.

Acknowledgements

The authors gratefully acknowledge financial support from the National Science Council of Taiwan (NSC 100-2112-M-019-002-MY3, 98-2119-M-002-007-MY3, 100-2119-M-007-010-MY3).

Received: October 5, 2012
Revised: December 6, 2012
Published online: January 22, 2013

[1] a) C. W. Tang, S. A. VanSlyke, *Appl. Phys. Lett.* **1987**, *51*, 913; b) C. Adachi, M. A. Baldo, S. R. Forrest, M. E. Thompson, *Appl. Phys. Lett.* **2000**, *77*, 904; c) M. A. Baldo, S. Lamansky, P. E. Burrows, M. E. Thompson, S. R. Forrest, *Appl. Phys. Lett.* **1999**, *75*, 4; d) Y. Sun, N. C. Giebink, H. Kanno, B. Ma, M. E. Thompson, S. R. Forrest, *Nature* **2006**, *440*, 908; e) S. Reineke, F. Lindner, G. Schwartz, N. Seidler, K. Walzer, B. Lussem, K. Leo, *Nature* **2009**, *459*, 234; f) C. Adachi, M. A. Baldo, S. R. Forrest, S. Lamansky, M. E. Thompson, R. C. Kwong, *Appl. Phys. Lett.* **2001**, *78*, 1622.

[2] M. A. Baldo, D. F. O'Brien, Y. You, A. Shoustikov, S. Sibley, M. E. Thompson, S. R. Forrest, *Nature* **1998**, *395*, 151.

[3] a) W. S. Jeon, T. J. Park, S. Y. Kim, R. Pode, J. Jang, J. H. Kwon, *Org. Electron.* **2009**, *10*, 240; b) A. Benor, S.-Y. Takizawa, C. Pérez-Bolivar, P. Anzenbacher, *Appl. Phys. Lett.* **2010**, *96*, 243310; c) H. Sasabe, Y.-J. Pu, K-i. Nakayama, J. Kido, *Chem. Commun.* **2009**, 6655; d) C. Han, G. Xie, H. Xu, Z. Zhang, D. Yu, Y. Zhao, P. Yan, Z. Deng, Q. Li, S. Liu, *Chem. Eur. J.* **2011**, *17*, 445; e) C. Han, Y. Zhao, H. Xu, J. Chen, Z. Deng, D. Ma, Q. Li, P. Yan, *Chem. Eur. J.* **2011**, *17*, 5800.

[4] a) Y. Tao, C. Yang, J. Qin, *Chem. Soc. Rev.* **2011**, *40*, 2943; b) A. Chaskar, H.-F. Chen, K.-T. Wong, *Adv. Mater.* **2011**, *23*, 3876; c) D. Yu, Y. Zhao, H. Xu, C. Han, D. Ma, Z. Deng, S. Gao, P. Yan, *Chem. Eur. J.* **2011**, *17*, 2592.

[5] a) D. Yu, F. Zhao, C. Han, H. Xu, J. Li, Z. Zhang, Z. Deng, D. Ma, P. Yan, *Adv. Mater.* **2012**, *24*, 509; b) C. Han, Z. Zhang, H. Xu, J. Li, G. Xie, R. Chen, Y. Zhao, W. Huang, *Angew. Chem., Int. Ed.* **2012**, *51*, 10104.

[6] a) H.-H. Chou, C.-H. Cheng, *Adv. Mater.* **2010**, *22*, 2468; b) S. Gong, Y. Chen, J. Luo, C. Yang, C. Zhong, J. Qin, D. Ma, *Adv. Funct. Mater.* **2011**, *21*, 1168; c) S.-J. Su, C. Cai, J. Kido, *Chem. Mater.* **2011**, *23*, 274; d) W.-Y. Hung, L.-C. Chi, W.-J. Chen, E. Mondal, S.-H. Chou, K.-T. Wong, Y. Chi, *J. Mater. Chem.* **2011**, *21*, 19249; e) M.-S. Lin, L.-C. Chi, H.-W. Chang, Y.-H. Huang, K.-C. Tien, C.-C. Chen, C.-H. Chang, C.-C. Wu, A. Chaskar, S.-H. Chou, H.-C. Ting, K.-T. Wong, Y.-H. Liu, Y. Chi, *J. Mater. Chem.* **2012**, *22*, 870; f) H.-F. Chen, L.-C. Chi, W.-Y. Hung, W.-J. Chen, T.-Y. Hwu, Y.-H. Chen, S.-H. Chou, E. Mondal, Y.-H. Liu, K.-T. Wong, *Org. Electron.* **2012**, *13*, 2671; g) W.-Y. Hung, G.-M. Tu, S.-W. Chen, Y. Chi, *J. Mater. Chem.* **2012**, *22*, 5410; h) S.-J. Su, C. Cai, J. Kido, *J. Mater. Chem.* **2012**, *22*, 3347; i) C. Han, Z.g Zhang, H. Xu, S. Yue, J. Li, P. Yan, Z. Deng, Y. Zhao, P. Yan, S. Liu, *J. Am. Chem. Soc.* **2012**, *134*, 19179; j) C. Han, Z. Zhang, H. Xu, G. Xie, J. Li, Y. Zhao, Z. Deng, S. Liu, P. Yan, *Chem. Eur. J.* **2013**, *19*, 141.

[7] a) X. Xu, S. Chen, G. Yu, C. Di, H. You, D. Ma, Y. Liu, *Adv. Mater.* **2007**, *19*, 1281; b) W.-Y. Hung, T.-C. Tsai, S.-Y. Ku, L.-C. Chi, K.-T. Wong, *Phys. Chem. Chem. Phys.* **2008**, *10*, 5822; c) S.-Y. Ku, W.-Y. Hung, C.-W. Chen, S.-W. Yang, E. Mondal, Y. Chi, K.-T. Wong, *Chem. Asian J.* **2012**, *7*, 133; d) M.-S. Lin, S.-J. Yang, H.-W. Chang, Y.-H. Huang, Y.-T. Tsai, C.-C. Wu, S.-H. Chou, E. Mondal, K.-T. Wong, *J. Mater. Chem.* **2012**, *22*, 16114.

[8] a) G. Hughes, M. R. Bryce, *J. Mater. Chem.* **2005**, *15*, 94; b) J. Lee, N. Chopra, S.-H. Eom, Y. Zheng, J. Xue, F. So, J. Shi, *Appl. Phys. Lett.* **2008**, *93*, 123306; c) H. Xia, M. Li, D. Lu, C. Zhang, W. Xie, X. Liu, B. Yang, Y. Ma, *Adv. Funct. Mater.* **2007**, *17*, 1757.

[9] N. Fomina, S. E. Bradforth, Th. E. Hogen-Esch, *Macromolecules* **2009**, *42*, 6440.

[10] P. E. Eaton, G. R. Carlson, J. T. Lee, *J. Org. Chem.* **1973**, *38*, 4071.

[11] F.-M. Hsu, C.-H. Chien, C.-F. Shu, C.-H. Lai, C.-C. Hsieh, K.-W. Wang, P.-T. Chou, *Adv. Funct. Mater.* **2009**, *19*, 2834.

[12] P.-I. Shih, C.-L. Chiang, A. K. Dixit, C.-K. Chen, M.-C. Yuan, R.-Y. Lee, C.-T. Chen, E. W.-G. Diau, C.-F. Shu, *Org. Lett.* **2006**, *8*, 2799.

[13] a) J. He, H. Liu, Y. Dai, X. Ou, J. Wang, S. Tao, X. Zhang, P. Wang, D. Ma, *J. Phys. Chem. C* **2009**, *113*, 6761; b) M. Sonntag, P. Strohriegl, *Chem. Mater.* **2004**, *16*, 4736; c) G. Zotti, G. Schiavon, S. Zecchin, J.-F.Morin, M. Leclerc, *Macromolecules* **2002**, *35*, 2122.

[14] M. Borsenberger, D. S. Weiss, in *Organic Photoreceptors for Imaging Systems*, New York **1993**, and references therein.

[15] a) C. Adachi, R. C. Kwong, P. Djurovich, V. Adamovisch, M. A. Baldo, M. E. Thompson, S. R. Forrest, *Appl. Phys. Lett.* **2001**, *79*, 2082; b) Y. Kawamura, K. Goushi, J. Brooks, J. J. Brown, H. Sasabe, C. Adachi, *Appl. Phys. Lett.* **2005**, *86*, 071104; c) N. Chopra, J. Lee, Y. Zheng, S. H. Eom, J. Xue, F. So, *Appl. Phys. Lett.* **2008**, *93*, 143307.

[16] C. Adachi, M. A. Baldo, M. E. Thompson, S. R. Forrest, *J. Appl. Phys.* **2001**, **90**, 5048.

[17] S.-J. Su, H. Sasabe, T. Takeda, J. Kido, *Chem. Mater.* **2008**, *20*, 1691.

[18] Y.-L. Tung, S.-W. Lee, Y. Chi, Y.-T. Tao, C.-H. Chien, Y.-M. Cheng, P.-T. Chou, S.-M. Peng, C.-S. Liu, *J. Mater. Chem.* **2005**, *15*, 460.

[19] a) W.-Y. Hung, L.-C. Chi, W.-J. Chen, Y.-M. Chen, S.-H. Chou, K.-T. Wong, *J. Mater. Chem.* **2010**, *20*, 10113; b) M.-T. Kao, W.-Y. Hung, Z.-H. Tsai, H.-W. You, H.-F. Chen, Y. Chi, K.-T. Wong, *J. Mater. Chem.* **2011**, *21*, 1846; c) W.-Y. Hung, H.-W. You, F.-C. Fan, H.-F. Chen, K.-T. Wong, *Org. Electron.* **2011**, *12*, 575.

[20] a) S.-J. Su, E. Gonmori, H. Sasabe, J. Kido, *Adv. Mater.* **2008**, *20*, 4189; b) Y.-Y. Lyu, J. Kwak, W. S. Jeon, Y. Byun, H. S. Lee, D. Kim, C. Lee, K. Char, *Adv. Funct. Mater.* **2009**, *19*, 420.

[21] L. Xiao, S.-J. Su, Y. Agata, H. Lan, J. Kido, *Adv. Mater.* **2009**, *21*, 1271.

[22] a) S. Chen, G. Tan, W.-Y. Wong, H.-S. Kwok, *Adv. Funct. Mater.* **2011**, *21*, 3785; b) Y.-S. Park, J.-W. Kang, D.-M. Kang, J.-W. Park, Y.-H. Kim, S.-K. Kwon, J.-J. Kim, *Adv. Mater.* **2008**, *20*, 1957.

[23] S. Gong, Y. Chen, C. Yang, C. Zhong, J. Qin, D. Ma, *Adv. Mater.* **2010**, *22*, 5370.

[24] a) G. Zhou, W.-Y. Wong, S. Suo, *J. Photochem. Photobiol. C: Photochem. Rev.* **2010**, *11*, 133; b) Q. Wang, D. Ma, *Chem. Soc. Rev.* **2010**, *39*, 2387; c) C. Han, G. Xie, H. Xu, Z. Zhang, L. Xie, Y. Zhao, S. Liu, W. Huang, *Adv. Mater.* **2011**, *23*, 2491.